J. Chem. Sci. Vol. 126, No. 2, March 2014, pp. 481–486.

CO_2 hydrogenation to hydrocarbons over iron nanoparticles supported on oxygen-functionalized carbon nanotubes

LY MAY CHEW, HOLGER RULAND, HENDRIK J SCHULTE, WEI XIA and MARTIN MUHLER*

Laboratory of Industrial Chemistry, Ruhr-University Bochum, 44780 Bochum, Germany
e-mail: muhler@techem.rub.de

MS received 22 October 2013; revised 3 January 2014; accepted 6 January 2014

Abstract. Hydrogenation of CO_2 to hydrocarbons over iron nanoparticles supported on oxygen-functionalized multi-walled carbon nanotubes was studied in a fixed-bed U-tube reactor at 25 bar with a H_2:CO_2 ratio of 3. Conversion of CO_2 was approximately 35% yielding C_1–C_5 products at 360°C with methane and CO as major products. The CO_2 equilibrium conversion for temperatures in the range of 320° to 420°C was analysed by using CHEMCAD simulation software. Comparison between experimental and simulated degrees of CO_2 conversion shows that reverse water gas shift equilibrium had been achieved in the investigated temperature range and that less than 47% of CO_2 can be converted to CO at 420°C.

Keywords. CO_2 hydrogenation; iron-based catalyst; multi-walled carbon nanotubes; equilibrium conversion.

1. Introduction

It is generally accepted that a high concentration of CO_2 has a huge impact on the environment, as the increase in the global temperature is caused by the rise in CO_2 emission.[1] Additionally, depletion in crude oil resources and continuous increase of its price have raised the interest in CO_2 hydrogenation.[2] Numerous research efforts have been made to convert CO_2 to valuable industrial feedstock rather than treating it as a waste. Among the CO_2 utilization methods, catalytic hydrogenation of CO_2 to hydrocarbons has gained much attention,[1,3] which has been known for several decades.[4] At present, hydrogenation of CO_2 can be viewed as an alternative process to produce high quality fuels without sulphur and aromatic compounds, because the product distribution obtained from CO_2 hydrogenation using iron-based catalysts is reported to be similar to Fischer–Tropsch Synthesis (FTS).[5] FTS is a well-established industrial process, in which synthetic gas (CO + H_2) is converted into mainly linear hydrocarbons with a broad chain-length distribution.[6,7] However, FTS releases considerable amounts of CO_2 due to the formation of CO_2 via the water gas shift reaction.[8,9] Hence, with concerns about global warming, CO_2 hydrogenation using H_2 from sustainable sources is considered as one of the promising methods to help reduce CO_2 emissions by converting CO_2 into valuable chemicals.

*For correspondence

CO_2 hydrogenation is assumed to occur in two consecutive steps: the reverse water gas shift reaction (RWGS) and FTS as described in eqs 1 and 2, respectively.[10–12]

$$\begin{aligned} \text{RWGS}: CO_2 + H_2 &= CO + H_2O \\ \Delta_R H_{573K} &= +38\ \text{kJ/mol}. \end{aligned} \quad (1)$$

$$\begin{aligned} \text{FTS}: nCO + (2n+1)H_2 &\rightarrow C_nH_{2n+2} + nH_2O \\ \Delta_R H_{573K} &= -166\ \text{kJ/mol}. \end{aligned} \quad (2)$$

CO is produced by RWGS as an intermediate product, which is subsequently hydrogenated to hydrocarbons by FTS. The main products of FTS are linear paraffins and α-olefins. Common by-products are oxygenates such as alcohols and aldehydes.[2,11] In recent years, several research groups have been working on CO_2 hydrogenation to hydrocarbons.[3,13–16] These studies were performed mostly over traditional FTS catalysts such as cobalt- and iron-based catalysts. CO_2 hydrogenation over cobalt-based catalysts produces mainly methane. The low water gas shift (WGS) activity was claimed to be responsible for the poor selectivity to FT products. Conversely, iron-based catalysts possess a higher WGS activity and are therefore more suitable for CO_2 hydrogenation.[5,15,17] It is well-known that magnetite is responsible for the RWGS reaction, whereas iron carbide is highly catalytically active for FTS.[11,12] Recently, carbon nanotubes (CNTs) have been

claimed as a promising support for catalysts used in FTS,[18–20] because CNTs have a large surface area and are able to improve the dispersion of catalytically active nanoparticles.[17] Oxygen functionalization of the exposed graphitic CNT surfaces is required to provide strong anchoring sites for the deposited nanoparticles.[21]

Here, we report CO_2 hydrogenation to hydrocarbons over iron nanoparticles supported on oxygen-functionalized CNTs (OCNTs). The iron catalyst was prepared by the incipient wetness impregnation method and the catalytic performance of the catalyst was examined in a fixed-bed U-tube reactor. In addition, the equilibrium CO_2 conversion, which was calculated using CHEMCAD software, was compared to the experimental CO_2 conversion to assess thermodynamic equilibrium limitations in the RWGS reaction.

2. Experimental

2.1 *Catalyst preparation*

Multi-walled CNTs with inner diameters of 20–50 nm and outer diameters of 70–200 nm were obtained from Applied Sciences Inc. (Ohio). As-received CNTs were subjected to nitric acid vapour originating from boiling concentrated nitric acid (65%) at 200°C for 24 h to create oxygen-containing functional groups.[21] The obtained OCNT samples were loaded with iron by incipient wetness impregnation using ammonium ferric citrate (Fluka, 14.5–16% Fe basis) as iron precursor.[22] Briefly, OCNTs were added to the aqueous solution of ammonium ferric citrate. A theoretical Fe loading of 40 wt% was applied. After stirring for approximately 1 h, the mixture was dried at 50°C overnight. Subsequently, the solid product was collected and calcined at 300°C in synthetic air (20.5% N_2 in O_2) with a flow rate of 100 sccm for 90 min.

2.2 *Characterization*

Powder X-ray diffraction (XRD) patterns were recorded with a Panalytical MPD diffractometer using Cu K_α radiation in the 2Θ range of 10–70°. Atomic absorption spectroscopy (AAS) was used to determine the actual loading of iron on the catalyst.

2.3 *Continuous hydrogenation set-up*

A schematic diagram of the experimental set-up is shown in figure 1. CO_2 hydrogenation experiments were conducted in a fixed-bed U-tube reactor with an inner diameter of 8 mm. Ar (99.999%), H_2 (99.999%), CO (99.997%) and CO_2 (99.5%) were connected to the set-up. The additional line, which is indicated as mix, was used for calibration or additional tests. Five mass flow controllers (Brooks® Model 5850TR) were utilized to adjust the required flow rates of the inlet gases. The reactor unit was placed in a hot box. To prevent condensation of products, the hot box and additionally the transfer line of product stream to the gas chromatograph were thermostated at 180°C. The pressure of the reaction was controlled by a TESCOM™ back-pressure regulator, which allows a pressure variation between atmospheric pressure and 35 bar. Furthermore, the temperature of the reactor was measured by a thermocouple, which was located between the outer wall of the reactor and the oven, and the temperature was controlled by a Eurotherm temperature controller. For the catalytic test, the catalyst was diluted with silicon carbide in a weight ratio of 1:4 in order to obtain isothermal conditions. The catalyst was positioned between two plugs of quartz wool in the reactor.

Online gas analysis was performed with a Shimadzu gas chromatograph (GC) equipped with a thermal conductivity detector (TCD) and two flame ionization detectors (FID) using argon as internal standard. A schematic configuration of the GC application is shown in figure 2. The GC was equipped with four capillary columns (CP-PoraPLOT Q, CP-Molsieve 5A and CP-Al_2O_3/KCl). CP-PoraPLOT Q (labelled as Poraplot 1 and Poraplot 2) is able to separate components such as alcohols, hydrocarbons and halogenated compounds. CP-Molsieve 5A (labelled as Molsieve) is designed for the separation of permanent gases including H_2, CO, O_2, N_2, CH_4 and Ar. Furthermore, separation of light hydrocarbons can be attained by using CP-Al_2O_3/KCl (labelled as Alox). Additionally, the GC was installed with three heated Valco® sampling valves (labelled as Valco 1, Valco 2 and Valco 3). He was used as carrier gas, which carriers the gas samples taken by Valco 1 to the Alox column and simultaneously to the Poraplot column via Valco 2. Gas samples separated on the Alox column were analysed by the FID. On the other hand, samples taken by Valco 2 were analysed for permanent gases, alcohols as well as hydrocarbons by the TCD and FID in series. The Valco valves were controlled independently at pre-programmed times in order to separate permanent gases (in this case, CO, Ar, H_2 and CH_4) and the rest of the products (e.g., CO_2, C_{2+} hydrocarbons and alcohols), in which the former entered the Molsieve column, whereas the latter bypassed the Molsieve column.

Initially, the samples entered the Poraplot column and subsequently into the Molsieve column. After the permanent gases entered, the Molsieve column was switched offline, before CO_2 eluted from the Poraplot column. The components including H_2, Ar, CO and

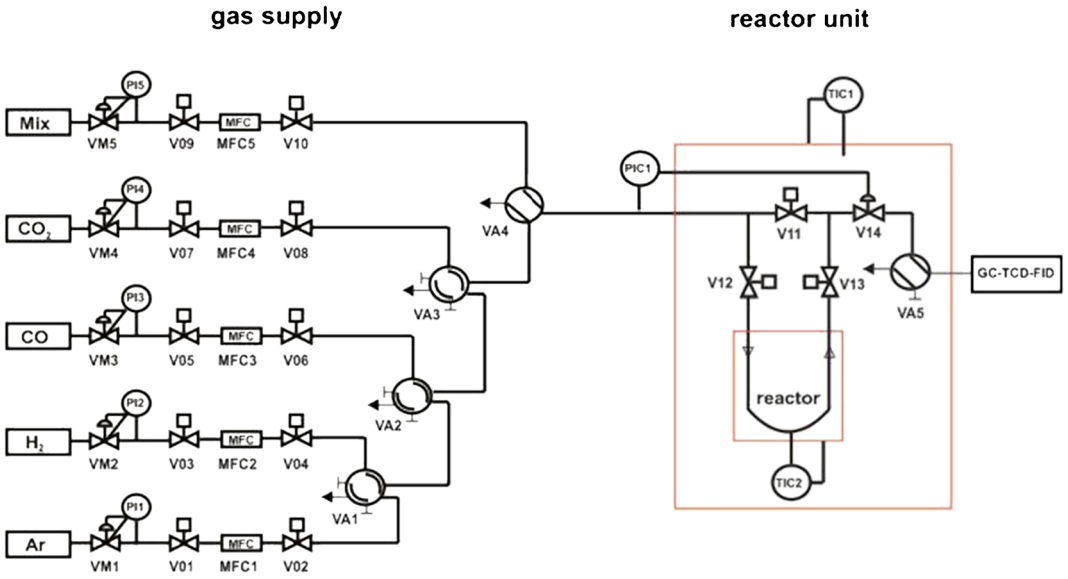

Figure 1. Schematic diagram of the set-up for CO_2 hydrogenation.

CH_4 were then retained on the Molsieve column. Instantly, CO_2, alcohols and hydrocarbons eluted from the Poraplot column bypassed the Molsieve column and reached the TCD and FID. Finally, the Molsieve column was switched online again and consequently the retained gases were eluted from the column and analysed by the detectors. A TCD was used to analyse permanent gases, whereas hydrocarbons and alcohols were analysed by the FID.

2.4 *Catalytic tests*

Typically, 240 mg of catalyst with 960 mg of silicon carbide were used in each CO_2 hydrogenation experiment. Prior to the catalytic tests, the catalyst was first reduced in pure H_2 at 380°C (2 K/min) and 25 bar for 5 h. Subsequently, the reactor was cooled to the reaction temperature of 360°C in flowing Ar. Afterwards, the hydrogenation reaction was performed at 360°C and

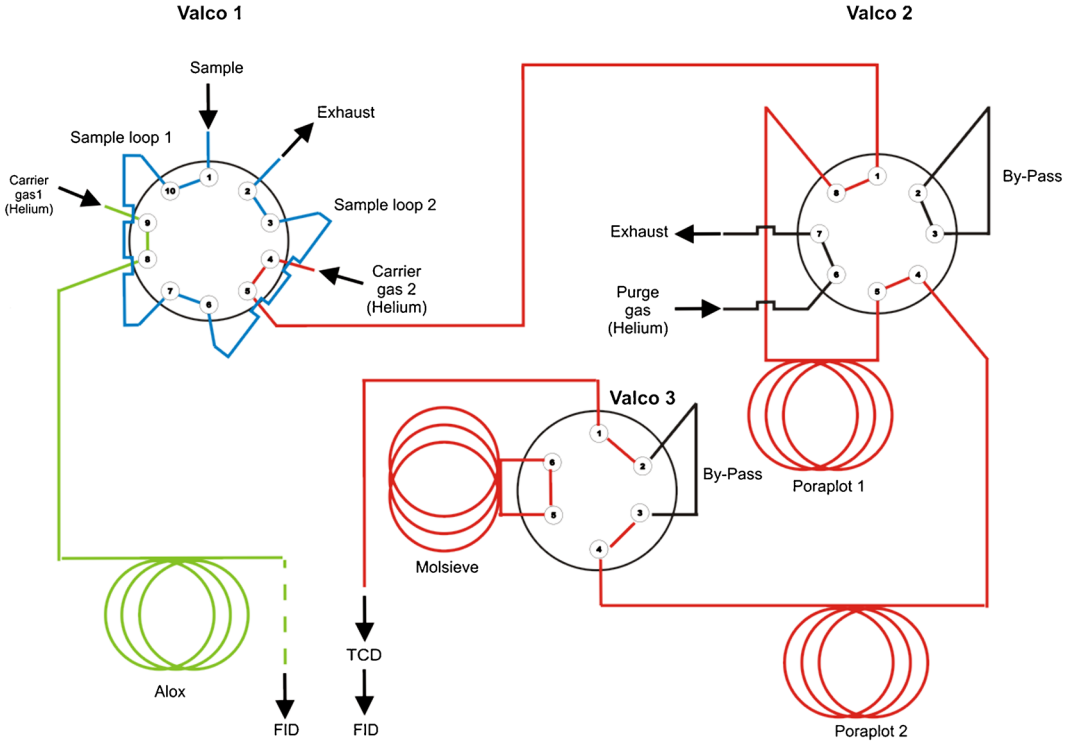

Figure 2. Schematic illustration of the online gas analysis performed by gas chromatography.

25 bar using a mixture of 22.5% CO_2, 67.5% H_2 and 10% Ar at a total flow rate of 8.333 L g^{-1} h^{-1}. The reaction was carried out for 50 h.

Additionally, a temperature variation experiment was conducted with the same pretreatment procedure. The reaction was first performed at 320°C, and subsequently the reaction temperature was set to 340°, 360°, 380°, 400° and 420°C. The reaction was held for approximately 24 h at each temperature in order to obtain steady-state conditions.

2.5 *Simulation*

Simulation was performed using the CHEMCAD software by Chemstations Inc.[23] Equilibrium conversion of CO_2 was determined by minimizing Gibbs free energy

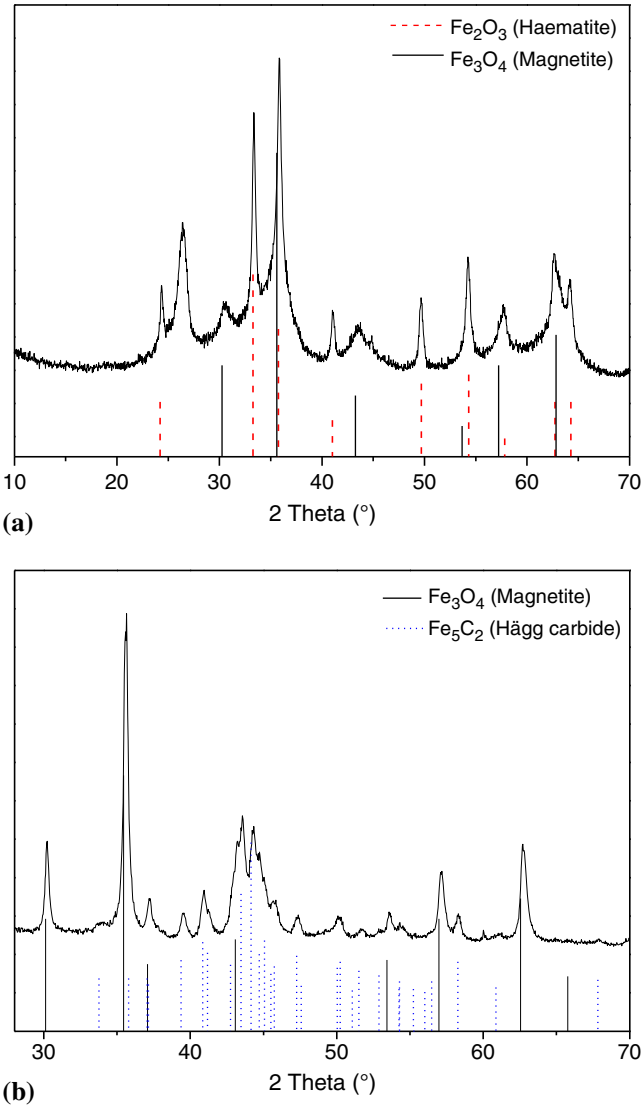

Figure 3. XRD patterns of (**a**) Fe/OCNT catalyst before reaction and (**b**) after reaction.

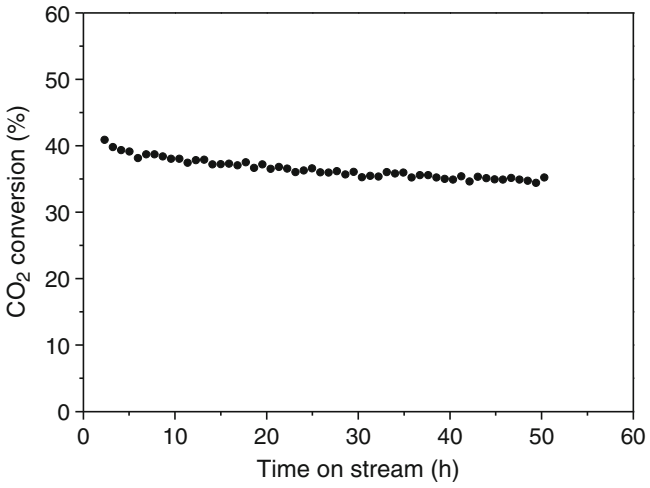

Figure 4. CO_2conversion as a function of time on stream. Reaction conditions: 360°C, 25 bar, $H_2/CO_2 = 3$, total flow of 8.333 L $g^{-1}h^{-1}$.

according to the given reactant composition and operating conditions. Furthermore, influence of the subsequent CO hydrogenation reaction on the preliminary RWGS equilibrium was considered to verify the experimental results. Simulation was performed to calculate equilibrium conversion of CO_2 at various temperatures in the range of 320° to 420°C.

3. Results and discussion

3.1 *Characterization of the catalyst*

Iron nanoparticles dispersed on the obtained OCNTs were synthesized by incipient wetness impregnation method using ammonium ferric citrate as precursor. The actual iron loading of the catalyst is determined by AAS to be 24.85 wt%. The XRD patterns of the Fe/OCNT catalyst before and after reaction are displayed in figure 3. The iron phases present in the catalyst before reaction were found to be haematite (Fe_2O_3) and magnetite (Fe_3O_4). In contrast, Hägg carbide (Fe_5C_2) and magnetite were observed in the catalyst after 50 h time on stream. It is well-known that magnetite is responsible for the RWGS reaction, whereas iron carbide is highly catalytically active for FTS.[11,12]

3.2 *Catalytic tests*

Catalytic activity of the Fe/OCNT catalyst was studied during CO_2 hydrogenation into short hydrocarbons. The degree of CO_2 conversion as a function of time on stream is shown in figure 4. The test was conducted in the continuous mode for 50 h at 360°C with a H_2:CO_2 ratio of 3 and at 25 bar with a total volumetric flow

Table 1. Product selectivity, olefin selectivity in the C_2–C_5 range and CO_2 conversion over the Fe/OCNT catalyst. Reaction conditions: 360°C, 25 bar, $H_2/CO_2 = 3$, total flow of 8.333 L $g^{-1}h^{-1}$.

	Product selectivity (%)									CO_2 conversion (%)
	Hydrocarbon						Alcohol			
Catalyst	CO	C_1	C_2	C_3	C_4	C_5	C_2	C_3	$C_{2=}$–$C_{5=}/C_{2-}$–C_{5-}	
Fe/OCNT	26.3	38.1	17.9	11.2	3.2	1.9	0.3	0.3	0.14	35.2

rate of 8.333 L $g^{-1}h^{-1}$. It can be seen from figure 4 that CO_2 conversion decreased initially and then slowly stabilized at about 35%.

Product selectivities, olefin selectivity and degrees of CO_2 conversion are summarized in table 1. About 35% of CO_2 were converted into C_1–C_5 products, mostly CO and methane, with selectivities around 26% and 38%, respectively. Olefin selectivity was only approximately 14% for the hydrocarbons range of C_2–C_5. This observation is in good agreement with studies reporting that using iron-based catalyst without promoters such as potassium and manganese resulted in high methane selectivity and low olefin to paraffin ratios.[5,13,17,24,25] Moreover, alkali promoters have the ability to increase the chain growth probability, thus favouring formation of long-chain hydrocarbons. It has been claimed that potassium enhances dissociative adsorption of CO and CO_2 and lowers H_2 adsorption ability.[26,27] It is known that oxygenates are common by-products in FTS. Indeed, small amounts of ethanol and 2-propanol were observed in the hydrogenation reaction (table 1). It was reported that alkali promoters are able to improve selectivity of oxygenates and the degree of alkalization has an influence on selectivity to oxygenates.[11] Hence, the catalyst will be optimized in this way to obtain high olefin selectivity and low methane formation.

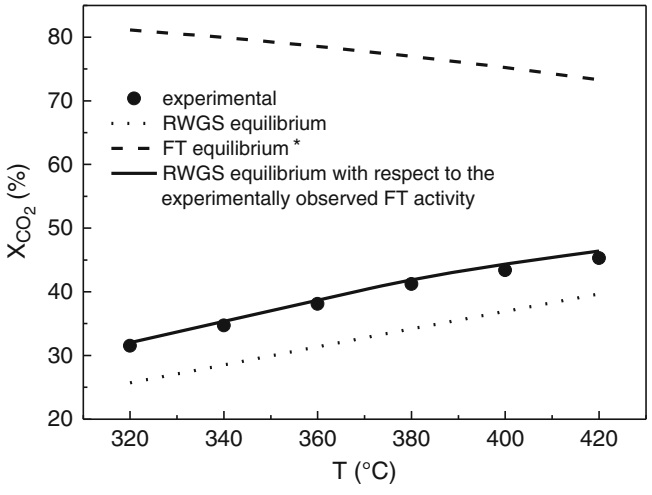

Figure 5. CO_2 equilibrium conversion and experimental CO_2 conversion as a function of temperature with 240 mg of Fe/OCNT catalyst at 25 bar and H_2:CO_2 = 3, total flow of 8.333 L $g^{-1}h^{-1}$, * C_2 and C_3 hydrocarbons were considered as possible products in the simulation.

3.3 *Simulation*

Equilibrium conversion of CO_2 at various temperatures was calculated using CHEMCAD software. Experimental and simulated degrees of CO_2 conversion are shown in figure 5. Simulation results indicate that RWGS equilibrium had been achieved in the experimental temperature range. Hence, CO_2 hydrogenation reaction is limited by RWGS (eq. 1) equilibrium under the applied conditions. Consequently, CO_2 conversion increases with increasing temperature as RWGS is a reversible endothermic reaction.

It can be seen that CO_2 equilibrium conversion (figure 5, solid line) with respect to the experimentally observed FT activity is higher than equilibrium conversion of the RGWS reaction (dotted line). Therefore, subsequent FT reaction plays an important role in the reaction network of CO_2 hydrogenation. Additional simulations including C_2 and C_3 hydrocarbons as possible products show the possibility of obtaining CO_2 conversions up to 80% (figure 5, dashed line): $CO_2 \rightarrow CO \rightarrow C_2 + C_3$. Results indicate that FTS (eq. 2) in CO_2

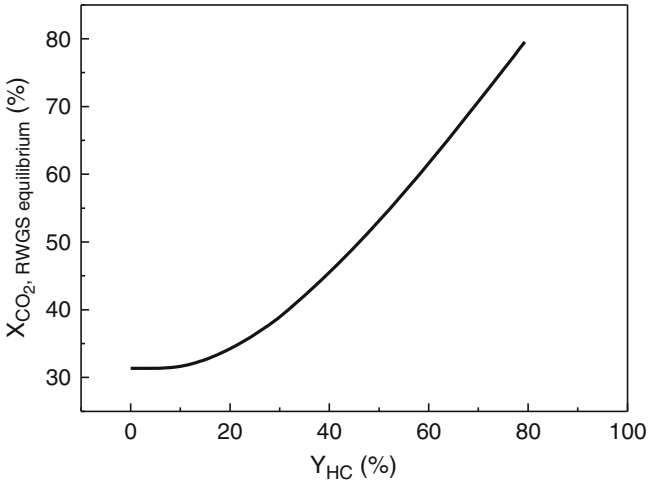

Figure 6. Simulated RWGS equilibrium as a function of the hydrocarbon yield at 360°C, 25 bar, H_2:CO_2 = 3, total flow of 8.333 L $g^{-1}h^{-1}$.

hydrogenation is a slow reaction compared with RWGS due to the low CO partial pressure.

Figure 6 demonstrates that CO_2 conversion with respect to RWGS equilibrium strongly increases with increasing hydrocarbon formation. This increase can be explained by a change in the partial pressure of the compounds involved in the RWGS reaction due to consumption of CO and H_2 and formation of H_2O in the FTS. Consequently, the position of RWGS equilibrium will change depending on FT activity. High degrees of CO_2 conversion can be achieved, when the catalyst is highly active in the subsequent FT reaction and formation of hydrocarbons reaches the equilibrium value as well. Hence, experimental conditions and catalyst will be optimized in order to achieve high yields of FT products in CO_2 hydrogenation.

4. Conclusions

Iron nanoparticles supported on OCNTs were prepared by incipient wetness impregnation method and used as catalyst in high temperature CO_2 hydrogenation. The experimental set-up was successfully used to perform the hydrogenation reaction. In addition, online GC analytics performed effectively in separating and analysing the products allowing us to close the carbon balance. Dominant iron phases on the catalyst under the operating conditions of CO_2 hydrogenation reaction were found to be Hägg carbide and magnetite by XRD measurements. Kinetic results demonstrate that CO_2 hydrogenation to short chain hydrocarbons is feasible using iron-based catalysts in spite of high methane formation and low olefin selectivity. Equilibrium conversion of CO_2 was calculated by using CHEMCAD software. Presence of equilibrium limitations for CO_2 conversion is verified by the simulation results indicating that RWGS equilibrium had been achieved in the temperature range of 320° to 420°C.

Acknowledgements

The study was conducted under the project 'Sustainable Chemical Synthesis (SusChemSys)', which is co-financed by the European Regional Development Fund (ERDF) and the state of North Rhine-Westphalia, Germany, under the Operational Programme 'Regional Competitiveness and Employment' 2007–2013.

References

1. Dorner R W, Hardy D R, Williams F W and Willauer H D 2010 *Energy Environ. Sci.* **3** 884
2. Laan G P D and Beenackers A 1999 *Catal. Rev.: Sci. Eng.* **41** 255
3. Riedel T, Schaub G, Jun K W and Lee K W 2001 *Ind. Eng. Chem. Res.* **40** 1355
4. Russell W W and Miller G H 1950 *J. Am. Chem. Soc.* **72** 2446
5. Riedel T, Claeys M, Schulz H, Schaub G, Nam S S, Jun K W, Choi M J, Kishan G and Lee K W 1999 *Appl. Catal.* **A186** 201
6. Dry M E 1996 *Appl. Catal.* **A138** 319
7. Schulz H 1999 *Appl. Catal.* **A186** 3
8. Ning W, Koizumi N and Yamada M 2009 *Energy Fuels* **23** 4696
9. Yao Y, Hildebrandt D, Glasser D and Liu X 2010 *Ind. Eng. Chem. Res.* **49** 11061
10. Dorner R W, Hardy D R, Williams F W, Davis B H and Willauer H D 2009 *Energy Fuels* **23** 4190
11. Riedel T, Schulz H, Schaub G, Jun K W, Hwang J S and Lee K W 2003 *Top. Catal.* **26** 41
12. Prasad P, Bae J W, Jun K W and Lee K W 2008 *Catal. Surv. Asia* **12** 170
13. Dorner R W, Hardy D R, Williams F W and Willauer H D 2010 *Energy Environ. Sci.* **3** 884
14. Ando H, Matsumura Y and Souma Y 2000 *J. Mol. Catal. A: Chem.* **154** 23
15. Choi P H, Jun K W, Lee S J, Choi M J and Lee K W 1996 *Catal. Lett.* **40** 115
16. Visconti C G, Lietti L, Tronconi E, Forzatti P, Zennaro R and Finocchio E 2009 *Appl. Catal.* **A355** 61
17. Dorner R W, Hardy D R, Williams F W and Willauer H D 2010 *Advances in CO_2 conversion and utilization* (Washington: American Chemical Society, ACS Symposium Series) Chapter 8 125
18. Tavasoli A, Sadagiana K, Khorashe F, Seifkordi A and Rohaniab A 2008 *Fuel Process. Technol.* **89** 491
19. Steen E and Prinsloo F F 2002 *Catal. Today* **71** 327
20. Schulte H J, Graf B, Xia W and Muhler M 2011 *Chem. Cat. Chem.* **4** 350
21. Xia W, Jin C, Kundu S and Muhler M 2009 *Carbon* **47** 919
22. Boot L A, Dillen A J, Geus J W and Buren F R 1996 *J. Catal.* **163** 186
23. Chemstations Inc., Houston, Texas, 2011
24. Cubeiro M L, Morales H, Goldwasser M R, Perez-Zurita M J, Gonzalez-Jimenez F and Nc C U 1999 *Appl. Catal.* **A189** 87
25. Cubeiro M L, Morales H, Goldwasser M R, Pérez-Zurita M J and González-Jiménez F 2000 *React. Kinetic Catal. Lett.* **69** 259
26. Dry M E, Shingles T, Boschoff L J and Oosthuizen G J 1969 *J. Catal.* **15** 190
27. Dorner R W, Hardy D R, Williams F W and Willauer H D 2010 *Appl. Catal.* **A373** 112